

ELEVATED-TEMPERATURE CREEP-FATIGUE CRACK-GROWTH BEHAVIOR OF NICKEL-BASED HAYNES® R-41, HAYNES® 230® and HASTELLOY® X ALLOYS

S.Y. Lee¹, P.K. Liaw¹, Y.L. Lu¹, D. Fielden¹, L.M. Pike² and D.L. Klarstrom²

¹Department of Materials Science and Engineering, The University of Tennessee, Knoxville, TN 37996, USA

²Haynes International, Inc., 1020 W. Park Ave., PO Box 9013, Kokomo, IN 46904, USA

Keywords: Fatigue-crack-growth, Hold time, Nickel-base HAYNES alloy

Abstract

The fatigue-crack-growth (FCG) experiments were performed on the nickel-base HAYNES R-41, HAYNES 230 and HASTELLOY X superalloys at temperatures ranging from 760°C to 927°C. The crack length was measured using a direct current potential drop technique. A triangular waveform of 0.333 Hz and a load ratio of 0.05 were employed under a constant-load-range control mode in the FCG tests. The various tensile hold times were imposed at the maximum load in the FCG tests to investigate fatigue and creep-fatigue interactions. It was found that the introduction of hold time and the increase of temperature led to a considerable increase in the cyclic-crack-growth rate. The fracture surfaces were investigated to determine the crack propagation mode using scanning electron microscope. Furthermore, the crack-growth rates of three superalloys were compared.

Introduction

Nickel-base superalloys are widely used for many high-temperature components in gas-turbine engines, power, chemical process, and industrial heating industries. They include both precipitation-strengthened alloys and solid-solution-strengthened alloys. The HAYNES R-41 alloy is a 58Ni-19Cr-11Co-10Mo (in weight percent) [1] precipitation-strengthened alloy that combines excellent high-temperature strength and good oxidation resistance. It has reasonable fabricability, although limited formability and issues such as strain-age cracking during post-weld heat treatments have often limited the application of the alloy in service. It is used in afterburner parts and nozzle diaphragm partitions in current gas-turbine engines. The HAYNES 230 (57Ni-22Cr-14W, in weight percent) [2] and HASTELLOY X (47Ni-22Cr-18Fe-9Mo, in weight percent) [3] are solid-solution-strengthened nickel-based superalloys. 230 alloy combines excellent high-temperature strength and oxidation resistance with a superior long term stability and good fabricability. X alloy possesses exceptional oxidation resistance, good fabricability, and excellent high-temperature strength. Both alloys are widely used in gas-turbine engines for combustion zone components.

One of the critical loading forms that lead to failures of these components is creep-fatigue, i.e., the combination of the time-dependent creep and cycle-dependent fatigue. Therefore, it is essential to investigate the fatigue-crack-propagation behavior with and without hold times for designing high-temperature components safely and finding the potential usages of alloys. In this study, crack-growth experiments with a tensile hold time at the maximum load were performed to study effects of the hold

time and test temperature on the crack-growth rates of the HAYNES R-41, HAYNES 230 and HASTELLOY X alloys. The fracture modes were determined with observation of scanning electron microscope. Moreover, the crack-growth rates of three superalloys were compared as a function of stress-intensity factor range (ΔK).

Experimental details

The compact-tension (CT) geometry chosen for the crack-growth tests is shown in Fig. 1. The thickness of the specimen was 3.2 mm. The height and width were 61.0 mm and 63.5 mm, respectively. The specimens were prepared according to the American Society for Testing and Materials (ASTM) Standards E647-99 [4].

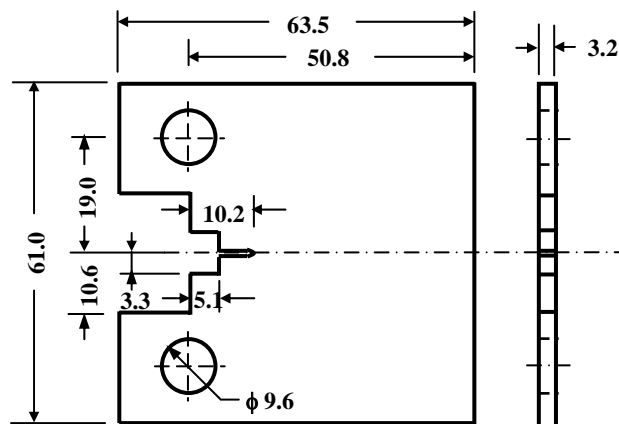


Fig. 1 The geometry of a compact-tension specimen (Unit: mm).

The crack-growth tests for R-41 alloy were conducted using a computer-controlled Material Test System (MTS) servohydraulic-testing machine. A resistance-type furnace was used to heat the specimen. The crack-growth tests for 230 and X alloys were conducted using an Instron servo-controlled, hydraulically-actuated, and closed-loop test machine. A high-frequency induction generator was used to heat the specimen. The fluctuation of the test temperature for three alloys was maintained within a range of $\pm 2^\circ\text{C}$. Prior to the crack-growth testing, CT specimens were precracked to approximately 1.27 mm at room temperature. A direct-current-potential-drop (DCPD) technique

was used to continuously monitor the crack length. The crack length is related to the electric potential by Johnson's equation [5].

$$\frac{V_m}{V_o} = \frac{\cosh^{-1}\left[\frac{\cosh(\pi y/W)}{\cos(\pi a/W)}\right]}{\cosh^{-1}\left[\frac{\cosh(\pi y_o/W)}{\cos(\pi a_o/W)}\right]} \quad (1)$$

where V_o and a_o are the initial crack-mouth potential and crack length, respectively, V_m and a are the instantaneous crack-mouth potential and crack length, respectively, y is half of the distance between the two points for which the crack-mouth potential is measured, and W is the specimen width. The stress-intensity factor, K , was obtained [6,7],

$$K = \frac{P}{BW^{1/2}} F(a/W) \quad (2)$$

where P = applied load, B = thickness, W = specimen width, and a = crack size for a CT specimen, and $\Delta K = K_{\max} - K_{\min}$. (K_{\max} and K_{\min} are the maximum and minimum stress-intensity factors, respectively).

$$F(a/W) = \frac{(2 + a/W)}{(1 - a/W)^{1.5}} f \quad (3)$$

$$f = 0.886 + 4.64a/W - 13.32(a/W)^2 + 14.72(a/W)^3 - 5.6(a/W)^4 \quad (4)$$

All crack-growth experiments were conducted under a constant-load-range control mode in laboratory air and at temperatures from 760°C to 927°C. A triangular waveform of 0.333 Hz and a load ratio of 0.05 were used in the fatigue crack-growth (FCG) tests. The creep-fatigue crack-growth (CFCG) tests were performed by superimposing the different hold time on the triangular waveform employed in the FCG tests at the maximum load.

Results and discussion

The cyclic-crack-growth rates, da/dN , for the R-41 alloy are presented as a function of the stress-intensity-factor range, ΔK , in Fig. 2.

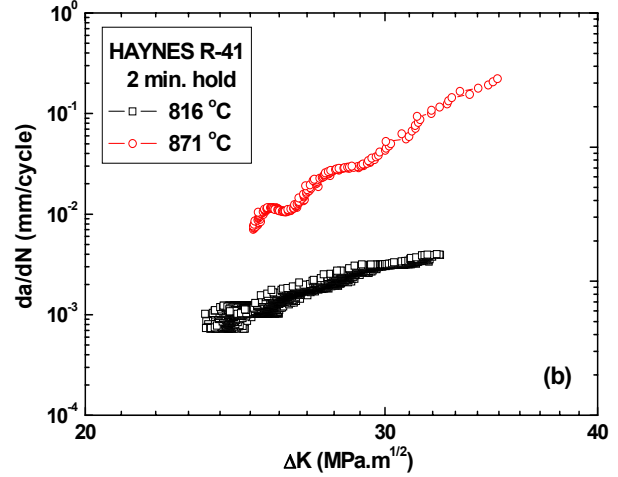
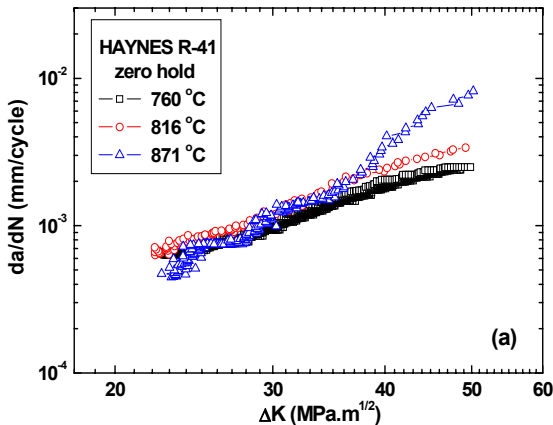


Fig. 2 Effects of the test temperature for the FCG tests (a) without hold time; (b) with 2 min.-hold time.

Figure 2(a) shows the effects of the test temperature for the FCG tests without hold times. As ΔK increases, the cyclic-crack-growth rate increased for all temperatures. The increase of the temperature from 760°C to 816°C resulted in a slight increase of the crack-growth rate in the ΔK investigated. When the test temperature increases from 816°C to 871°C, it was found that the crack-growth rate at 871°C was lower than that at 816°C below a ΔK of 30 $\text{MPa}\sqrt{\text{m}}$, and it was comparable in a ΔK from 30 $\text{MPa}\sqrt{\text{m}}$ to 37 $\text{MPa}\sqrt{\text{m}}$. However the crack-growth rate at 871°C was greater than that at 816°C above a ΔK of 37 $\text{MPa}\sqrt{\text{m}}$. It can be noted that the fatigue crack resistance at 871°C is the highest in the low ΔK region. The crack-growth rates of the FCG tests with a 2 min.-hold time at 816°C and 871°C are indicated in Fig. 2(b). As the temperature increases from 816°C and 871°C, the cyclic-crack-growth rates increased in all ΔK examined. For example, with a ΔK of 30 $\text{MPa}\sqrt{\text{m}}$, the cyclic-crack-growth rate at 871°C was about fifteen times greater than that at 816°C. Furthermore, the difference of the crack-growth rates at 816°C and 871°C increased with increasing ΔK .

Figure 3 shows the cyclic-crack-growth rates versus stress-intensity-factor range for 230 and X alloys at 816°C and 927°C. The effects of temperature for FCG tests without hold times are presented in Fig. 3(a). The increase of temperature for 230 alloy resulted in higher crack-growth rate in all ΔK . The crack growth rate of X alloy at 816°C was comparable to that at 927°C below a ΔK of 25 $\text{MPa}\sqrt{\text{m}}$, while the crack-growth rate at 927°C was greater than that at 816°C above a ΔK of 25 $\text{MPa}\sqrt{\text{m}}$. It is noted that the crack-growth rate of X alloy was higher than that of 230 alloy at both temperatures. Figure 3(b) shows the effects of temperature for FCG tests with 2 min.-hold time. The crack-growth rates in all ΔK increased significantly with increasing the test temperature. For instance, with a ΔK of 30 $\text{MPa}\sqrt{\text{m}}$, the cyclic-crack-growth rates at 927°C for 230 and X alloys were about fifty and thirty times greater than those at 816°C, respectively. Moreover, it was revealed that the crack-growth rates of X alloy for 2 min.-hold test are larger than those of 230 alloy in all ΔK regions.

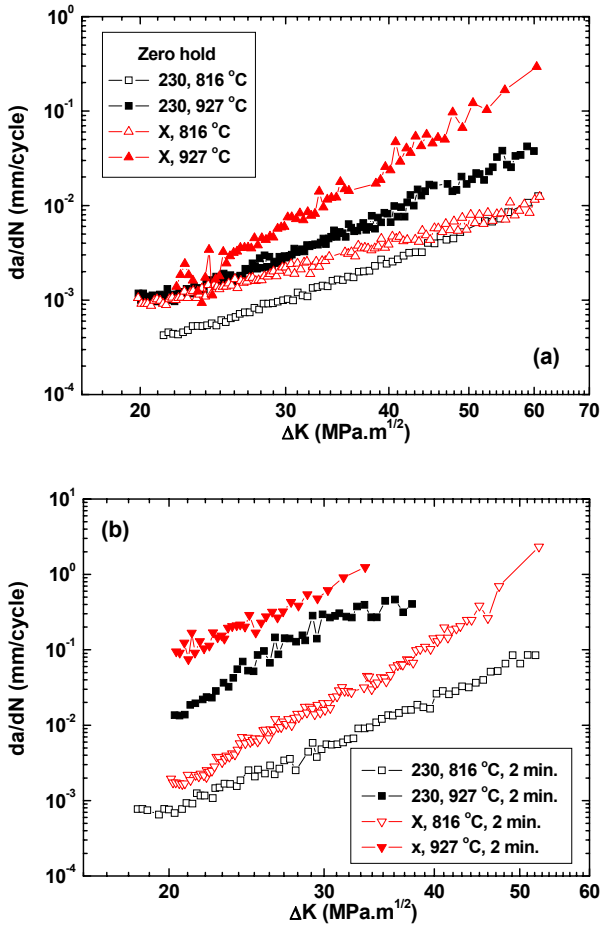


Fig. 3 Effects of the test temperature for the FCG tests (a) without hold time; (b) with 2 min.-hold time for 230 and X alloys.

The effects of the 2 min.-hold time for R-41 alloy at 816°C and 871°C are shown in Fig. 4(a). The introduction of a 2 min.-hold time at the maximum load significantly increased the crack-growth rate at both temperatures. The 2 min.-hold time test at 871°C resulted in much greater cyclic-crack-growth rate changes, as compared to that at 816°C. For instance, the cyclic-crack-growth rate of the 2 min.-hold test at 816°C was about three times greater than that of the zero-hold test at a ΔK of 30 $\text{MPa}\sqrt{\text{m}}$, while the cyclic-crack-growth rate of the 2 min.-hold test at 871°C was about forty times higher than that of the zero-hold test. Moreover, the differences between the continuous and hold-time crack-growth rates increased with increasing ΔK . Figure 4(b) shows the influence of the 2 min.-hold time on the crack-growth rate of 230 alloy. When a 2 min.-hold time was imposed, the crack-growth rates tremendously increased at both temperatures. The difference of crack-growth rate between the zero and 2 min.-hold time tests increased gradually with increasing ΔK . Figure 4(c) shows the changes of crack growth rate of X alloy with introduction of hold times at 816°C and 927°C. As the hold time increases, the crack-growth rate significantly increased at both temperatures. Especially, when a 60 min.-hold time was introduced at 816°C, the cyclic-crack-growth rate at a ΔK of 30

$\text{MPa}\sqrt{\text{m}}$ was about three hundred times greater than that of the zero-hold test.

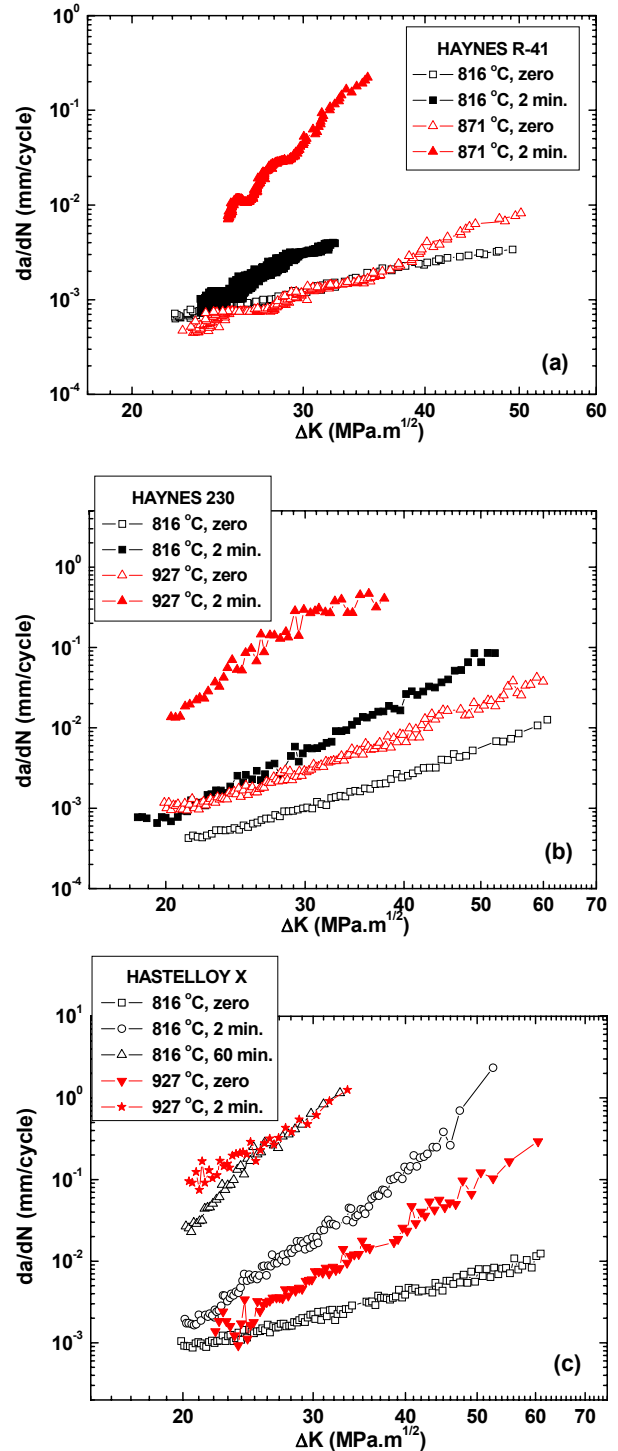


Fig. 4 The cyclic-crack growth rate as a function of ΔK for (a) R-41; (b) 230; (c) X alloys.

The fracture surfaces of 230 alloy after FCG tests were examined to evaluate the crack propagation mode using scanning electron microscope. Figure 5(a) presents that the crack propagated in a transgranular fracture mode showing well-defined fatigue striation for FCG test without hold time at 816°C. The secondary crack was often examined, suggesting that the grain boundary cavity would be developed by creep deformation although alloy is subjected to only fatigue loading. On the other hand, 2 min.-hold time resulted in a dominant intergranular fracture mode, as shown in Fig. 5(b). The fatigue striation is hardly observed. As temperature increases from 816°C to 927°C, the fracture mode was changed from transgranular to dominant intergranular (Fig. 5(c)). For test with 2 min.-hold time at 927°C (Fig. 5(d)), a complete intergranular fracture appearance was observed.

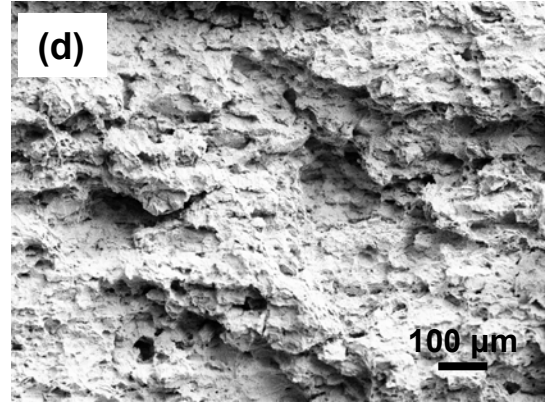
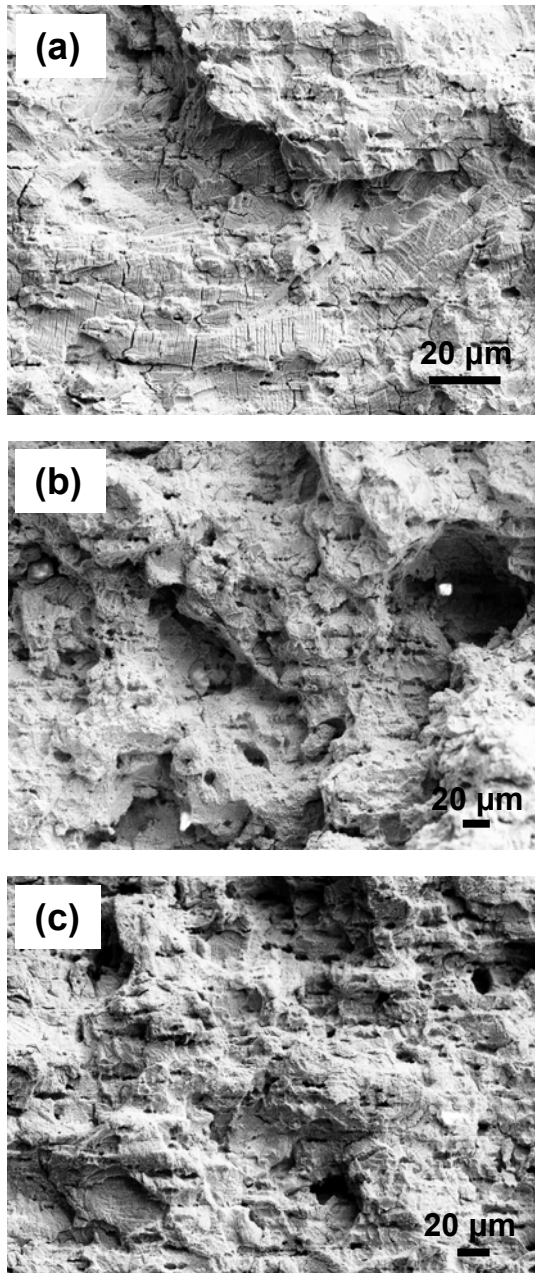


Fig. 5 SEM micrograph of the fracture surface at a ΔK of $35 \text{ MPa}\sqrt{\text{m}}$ for HAYNES 230 alloy: (a) 816°C, without hold time; (b) 816°C, 2 min.-hold time; (c) 927°C, without hold time; (d) 927°C, 2 min.-hold time.

Figure 6(a) shows the fracture surface of X alloy for test without hold time at 816°C and $\Delta K=23.5 \text{ MPa}\sqrt{\text{m}}$. A typical transgranular mode was examined indicating that crack propagated through the grain. When a 2 min.-hold time is imposed, the fracture mode is changed from transgranular to complete intergranular, as shown in Fig. 6(b). Figures 6(c) and 6(d) show an intergranular fracture feature for test with 60 min.-hold time, indicating that crack propagated along the grain boundary due to creep deformation. It is obvious that the time-dependent creep developed by the tensile hold time resulted in the intergranular cracking path. Figure 6(e) shows the dominant intergranular feature for the test without hold time at 927°C. It is noted that the increase of temperature resulted in the change of fracture mode and higher crack-growth rate (Fig. 3(a)). When 2 min.-hold time is introduced (Fig. 6(f)), the fracture mode was completely intergranular.

Based on analyses of fractography, as the temperature and hold time increase, it should be pointed out that the fracture mode changes from transgranular to intergranular feature. Intergranular fracture is caused by the time-dependent creep deformation. Higher temperature and longer hold time facilitate for the creep deformation accompanying the grain boundary cavitation. Consequently, it resulted in an intergranular fracture. From the previous crack growth studies with various hold times, it was found that the intergranular cracking path corresponds to the time-dependent cracking range and resulted in higher crack growth rate [8,9]. As a result, the increase of temperature and hold time would lead to higher crack growth rate developing an intergranular fracture due to creep deformation.

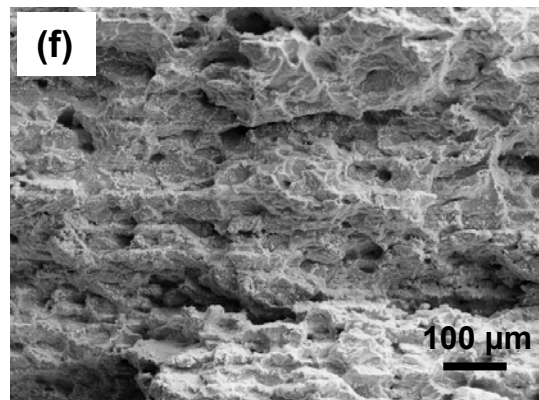
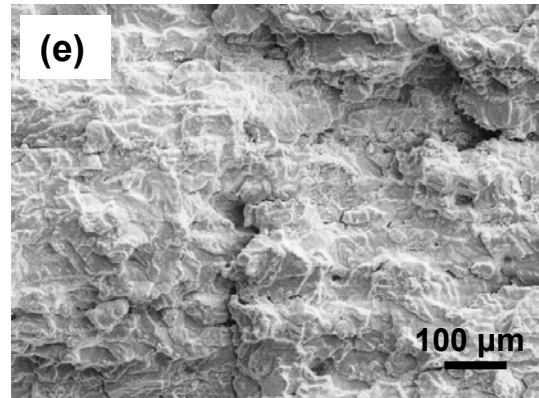
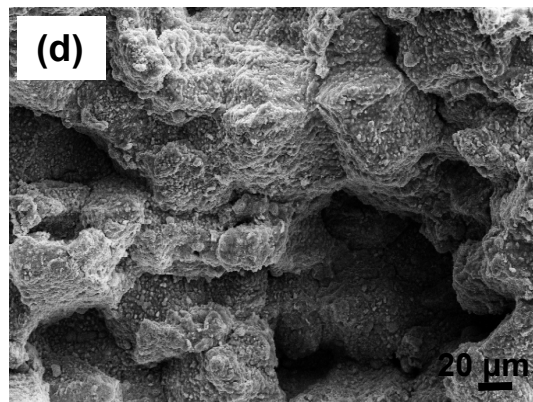
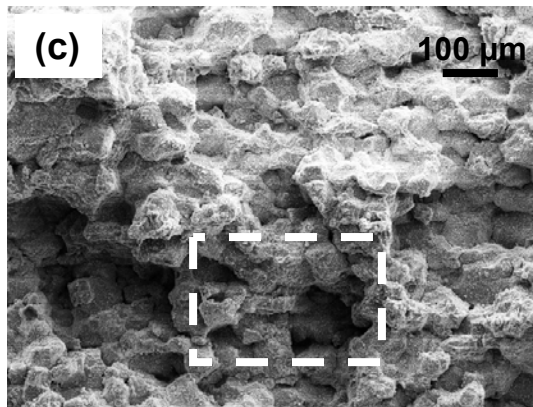
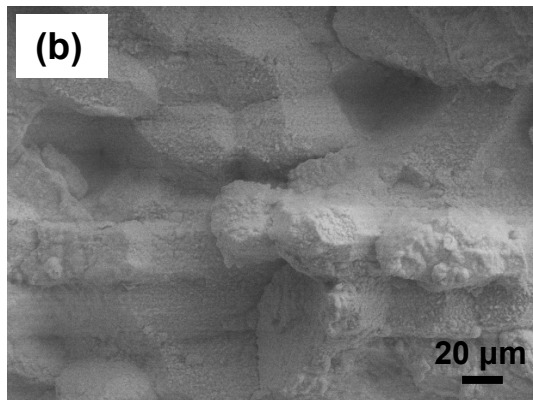
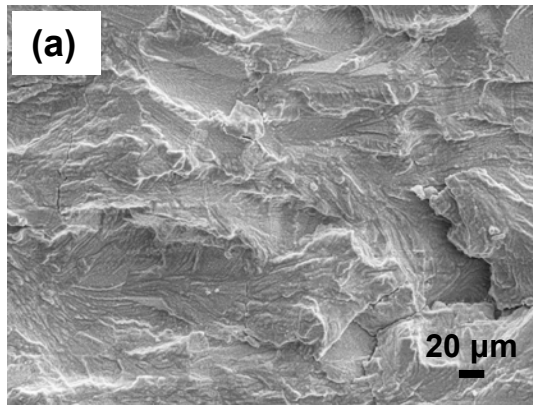


Fig. 6 SEM micrograph of the fracture surface for HASTELLOY X alloy: (a) 816°C, without hold time, $\Delta K=23.5 \text{ MPa}\sqrt{\text{m}}$; (b) 816°C, 2 min.-hold time, $\Delta K=23.5 \text{ MPa}\sqrt{\text{m}}$; (c) 816°C, 60 min.-hold time, $\Delta K=23.5 \text{ MPa}\sqrt{\text{m}}$; (d) higher magnification view of the rectangular area in (c); (e) 927°C, without hold time, $\Delta K=30 \text{ MPa}\sqrt{\text{m}}$; (f) 927°C, 2 min.-hold time; $\Delta K=30 \text{ MPa}\sqrt{\text{m}}$.

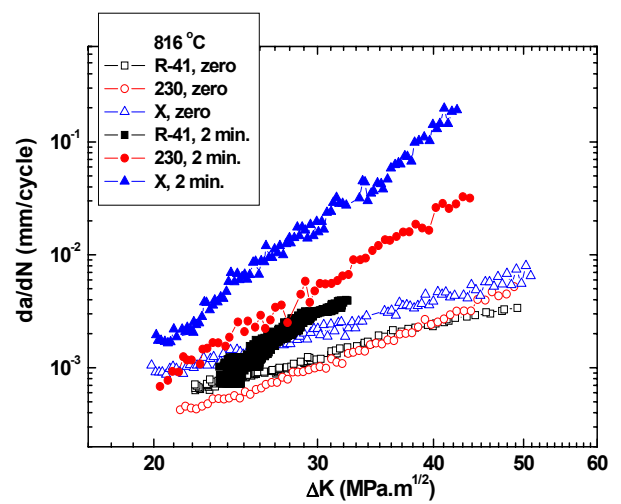


Fig. 7 Comparison of the cyclic-crack growth rates among the three alloys at 816°C.

The crack-growth rates of three nickel-based alloys were compared, as shown in Fig. 7. For the FCG tests without hold time at 816°C, the crack-growth rate of the X alloy was the highest among three alloys, and the R-41 and 230 alloys were very comparable. In the low ΔK region, the crack-growth rate of the 230 alloy is lower than that of the R-41 alloy, while the fatigue crack resistance of the R-41 alloy is greater than that of the 230 alloy in higher ΔK region. When a 2 min.-hold time was introduced, the creep-fatigue resistance of the R-41 alloy was the most superior, followed by the 230 alloy, and then the X alloy. It is thought that the different crack-growth rates of three alloys would be caused by distinct creep-resistance of materials. In further work, the examination of fracture mode of R-41 alloy with and without hold times will be performed and its influence of crack-growth rates will be compared with other two alloys.

Summary

The fatigue-crack-growth experiments with and without hold times were conducted at temperatures ranging from 760°C to 927°C. The increase of the temperature and the introduction of hold times resulted in the change of fracture mode from transgranular to intergranular and a substantial increase in the crack-growth rates. The difference of the crack-growth rates increased with increasing ΔK . Furthermore, the crack-growth rates of three superalloys were compared. The creep-fatigue resistance with the introduction of 2 min.-hold time of the HAYNES R-41 alloy was the best, followed by the HAYNES 230 alloy, and then the HASTELLOY X alloy.

Acknowledgements

This work is supported by the Haynes International, Inc., the National Science Foundation (NSF) Combined Research-Curriculum Development (CRCDD) Programs, under EEC-9527527 and EEC-0203415, the Integrative Graduate Education and Research Training (IGERT) Program, under DGE-9987548, and the International Materials Institutes (IMI) Program under DMR-0231320, with Dr. D. Durham, Ms. M. Poats, Dr. C. J. Van Hartesveldt, Dr. D. Dutta, Dr. W. Jennings, Dr. L. Goldberg, and Dr. C. Huber of NSF as program directors.

References

- Haynes online literature, No. H-3056, HAYNES R-41 alloy brochure: <http://www.haynesintl.com>
- Y.L. Lu, L.J. Chen, P.K. Liaw, G.Y. Wang, C.R. Brooks, S.A. Thompson, J.W. Blust, P.F. Browning, A.K. Bhattacharya, J.M. Aurrecochea, D.L. Klarstrom, "Effects of Temperature and Hold Time on Creep-Fatigue Crack-Growth Behavior of HAYNES[®] 230[®] Alloy", *Materials Science and Engineering A*, 429 (2006), 1-10.
- Y.L. Lu, P.K. Liaw, L.J. Chen, G.Y. Wang, M.L. Benson, S.A. Thompson, J.W. Blust, P.F. Browning, A.K. Bhattacharya, J.M. Aurrecochea, D.L. Klarstrom, "Tensile-Hold Effects on High-Temperature Fatigue-Crack-Growth in Nickel-Based HAYSTELLOY[®] X Alloy", *Materials Science and Engineering A*, 433 (2006), 114-120.
- ASTM Standard E 647-99: "Standard Test Method for Measurement of Fatigue Crack Growth Rates," 2000 Annual Book of ASTM Standards, Vol. 03.01, 591-630.
- H.H. Johnson, "Calibrating Electric Potential Method for Studying for Slow Crack Growth", *Materials Research and Standards*, 5 (1965) 442-445.
- H. Tada, P.C. Paris, and G.R. Irwin, "Stress Analysis of Cracks Handbook", Del Research Co., St. Louis (1985).
- D.P. Rooke and D.J. Cartwright, "Compendium of Stress Intensity Factors", Her Majesty's Stationery Office, London (1976).
- S.Y. Lee, Y.L. Lu, P.K. Liaw, S.A. Thompson, J.W. Blust, P.F. Browning, A.K. Bhattacharya, J.M. Aurrecochea, and D.L. Klarstrom, "Elevated-Temperature Low-Cycle-Fatigue and Crack-Propagation Behaviors of HAYNES[®] 230[®] and HASTELLOY[®] X alloys", 7th International Charles Parsons Turbine Conference (Parsons 2007), Glasgow, UK, September 11-13, (2007) 173-180.
- S.Y. Lee, Y.L. Lu, P.K. Liaw, H. Choo, S.A. Thompson, J.W. Blust, P.F. Browning, A.K. Bhattacharya, J.M. Aurrecochea, and D.L. Klarstrom, "High-Temperature Tensile-Hold Crack-Growth Behavior of HASTELLOY[®] X Alloy Compared to HAYNES[®] 188 and HAYNES[®] 230[®] Alloys", *Mechanics of Time-Dependent Materials*, 12 (2008), 31-44.